International Journal of Biological Macromolecules 48 (2011) 398–402

Contents lists available at ScienceDirect

International Journal of Biological Macromolecules

journal homepage: www.elsevier.com/locate/ijbiomac

Conformational stability of peanut agglutinin using small angle X-ray scattering

Patricia Targon Campana [a,*], Leandro Ramos Souza Barbosa [b], Rosangela Itri [b]

[a] Escola de Artes, Ciências e Humanidades da Universidade de São Paulo, Av. Arlindo Bettio, 1000 Ermelino Matarazzo, CEP 03828-000 São Paulo, SP, Brazil
[b] Departamento de Física Aplicada do Instituto de Física da Universidade de São Paulo, Caixa Postal 66318, CEP: 05315-970, São Paulo - SP, Brazil

ARTICLE INFO

Article history:
Received 29 September 2010
Received in revised form 7 December 2010
Accepted 9 December 2010
Available online 5 January 2011

Keywords:
PNA
Peanut lectin
Lectin
SAXS
Conformational stability

ABSTRACT

In this work, quaternary conformational studies of peanut agglutinin (PNA) have been carried out using small-angle X-ray scattering (SAXS). PNA was submitted to three different conditions: pH variation (2.5, 4.0, 7.4 and 9.0), guanidine hydrochloride presence (0.5–2 M) at each pH value, and temperature ranging from 25 to 60 °C. All experiments were performed in the absence and presence of T-antigen to evaluate its influence on the lectin stability. At room temperature and pH 4.0, 7.4 and 9.0, the SAXS curves are consistent with the PNA scattering in its crystallographic native homotetrameric structure, with monomers in a jelly roll fold, associated by non-covalent bonds resulting in an open structure. At pH 2.5, the results indicate that PNA tends to dissociate into smaller sub-units, as dimers and monomers, followed by a self-assembling into larger aggregates. Furthermore, the conformational stability under thermal denaturation follows the pH sequence 7.4 > 9.0 > 4.0 > 2.5. Such results are consistent with the conformational behavior found upon GndHCl influence. The presence of T-antigen does not affect the protein quaternary structure in all studied systems within the SAXS resolution.

1. Introduction

Lectins constitute a special class of proteins and glycoconjugates found in most organisms, ranging from viruses and bacteria to plants and animals. They have the ability to bind mono and oligosaccharides reversibly and with high specificity, but are devoid of catalytic activity. In contrast to antibodies, they are not products of an immune response, although several lectins are related to the activation of the human immune system, as the mannose binding lectins (MBL) and some leguminous lectins [1].

These molecules have come into the forefront of biological research, since they have been identified as carbohydrate-specific reagents and also biological recognition molecules. For this reason, a wide range of phenomena in which they are involved has been investigated as the structural and functional properties of complex carbohydrates, glycoproteins and glycolipids, the changes that occur on cell surfaces during physiological and pathological processes [2], the ability of inhibiting HIV-I and HIV-II (human immunodeficiency virus) replication [3], and in folding studies [4–7].

Lectins have also been used in tumoral cells recognition processes, due to their affinity to T-antigen [8,9]. Such an antigen, also known as Thomsen–Friedenreich antigen [10], makes part of tumor-associated carbohydrate antigens (TACAs) that have been used for cancer vaccines development. The main idea consists to immunize patients against TACAs, promoting an antibody response against tumoral cells [11,12]. This is due to the fact that the antigens are related to altered glycosylation patterns that can be considered as a tumor phenotype fingerprint. In this sense, lectins play an important role in the vaccines design due to their ability to differentiate carbohydrates and, consequently, to identify structural features related to malignant transformed tumor cells. Specifically, lectins with T-antigen affinity, as jacalin, amaranthin, scyllin-2 and peanut (*Arachis hypogea*) agglutinin, PNA, present a differential binding to malignant in respect to non-malignant cells [13–16].

In the current work, we focus our attention on the quaternary stability of the PNA due to its importance in the lectin binding to cell surface glycoconjugates when the adhesion or recognition is performed in a multivalent way. The PNA crystallographic structure, solved in 1996 by Bannerjee et al. [17], is a homotetrameric lectin, with monomers in a jelly roll fold, associated by non-covalent bonds resulting in an open structure. This quaternary structure is formed by association of two dimers, each one formed by the association of two monomer flat sheets. The folding of PNA has been previously studied and it seems that this non-usual quaternary structure provides to this lectin a completely different stability behavior in respect to those found for other legume lectins with similar folding [17]. Frutalin, e.g., a tetrameric lectin with β-sheet conformation, is completely unfolded upon addition of 4 M GndHCl at neutral pH [7], while PNA keeps the major part of its structure intact, only acquiring a completely unfolded state in the presence of 5 M GndHCl [18], as revealed by circular dichroism. In addition, the analysis of PNA chemical denaturation shows that this protein retains a significant secondary structure up to 5 M of urea at

* Corresponding author. Tel.: +55 11 3091 8883; fax: +55 11 3091 1020.
E-mail address: pcampana@usp.br (P.T. Campana).

0141-8130/
doi:10.1016/j.ijbiomac.2010.12.009

neutral pH [5]. Besides, dynamic light scattering (DLS) measurements reported on changes in PNA hydrodynamic radius, with a simultaneous molten globule formation, upon increasing urea concentration [19]. Further, studies focusing on the pH variation upon a trifluorethanol addition [20], reveal that the aromatic vicinities only change at pH around 2.5 with high trifluorethanol concentration.

Small angle X-ray scattering (SAXS) is a powerful technique to study protein stability in solution. For instance, SAXS technique was used to study the redox-active Concanavalin A, showing that the interaction between the lectin and the linkers that compose the electrodes does not alter significantly the protein conformation, preserving also its activity [21]. SAXS technique was also used to understand the oligomerization process of *Bothrops jararacussu* β-galactoside-specific C-type lectin. The authors observed that the oligomerization state, a decamer constituted by disulfide-linked homodimers, is biologically relevant for the envenoming event [22]. Furthermore, SAXS was also employed to characterize the quaternary structure of a new lectin referred to as camptosemin from *Camptosema ellipticum* [23]. In the present work, we investigate the quaternary conformational changes induced on the PNA structure by pH variation, guanidine hydrochloride presence, and temperature, by means of SAXS. The influence of T-antigen is also experienced in order to verify its role in PNA quaternary stability.

2. Materials and methods

2.1. Materials

Sodium acetate, sodium borate, sodium phosphate, peanut agglutinin, PNA (L0881), T-antigen and guanidine hydrochloride (GndHCl) were purchased from Sigma–Aldrich (St. Louis, MO) and used without any further purification. All solutions were prepared using ultrapure Milli-Q water and all reagents were of analytical grade.

2.2. Sample preparation

PNA stock solutions were prepared in a 20 mM sodium phosphate, sodium borate and sodium acetate (PBA) buffer at pH 2.5, 4.0, 7.4 and 9.0 in the presence and absence of GndHCl (0.5 and 2 M) and T-antigen at a molar ratio of 1:4 PNA:T-antigen. The final protein concentration was 10 mg/mL for all SAXS measurements.

2.3. SAXS experiments

SAXS experiments were performed at the National Synchrotron Light Laboratory (LNLS, Campinas, Brazil) at room temperature of 298 K, with radiation wavelength $\lambda = 1.488$ Å and sample-to-detector distance of 1360 mm, which enable collection of a scattering vector ($q = (4\pi/\lambda)\sin\theta$, being 2θ the scattering angle) ranging from $q_{min} = 0.015$ Å^{-1} to $q_{max} = 0.25$ Å^{-1}. According to the sampling theorem [24], the maximum dimension of scattering particle that could be achieved was circa 430 Å ($D_{max} = 2\pi/q_{min}$). Samples were set between two mica windows and a 1 mm spacer, handled in a liquid sample-holder, coupled to a temperature controller. This was placed perpendicular to the primary X-ray beam. The obtained curves (data collection of 10 min) were corrected for detector homogeneity (bi-dimensional position-sensitive detector) and normalized by taking into account the decrease of the X-ray beam intensity during the experiment. The parasitic background from the buffer solution was subtracted, considering the sample's attenuation. Samples were measured at room temperature (25 °C), 45 °C and 60 °C.

2.4. SAXS data analysis

It is well known that the scattering intensity, $I(q)$, from a set of non-interacting proteins randomly distributed in solution is proportional to the protein form factor, $P(q)$ [24,25]. A Fourier transform connects $I(q)$ to the pair distance distribution function, $p(r)$, which represents the probability of finding a pair of small elements at a distance r within the entire volume of the scattering particle, such that [24,25]:

$$p(r) = \left(\frac{1}{2\pi^2}\right)\int_0^\infty I(q)qr\sin(qr)dq \quad (1)$$

This function provides information about the scattering particle shape as well as its maximum dimension, D_{max}, accounted for a certain r value where $p(r)$ approaches to zero. Moreover, the radius of gyration R_g is calculated as:

$$R_g^2 = \frac{\int_0^{D_{max}} r^2 p(r)dr}{2\int_0^{D_{max}} p(r)dr} \quad (2)$$

In this work, $p(r)$ functions were calculated by means of the generalized indirect Fourier transform [26] software. Furthermore, the protein form factor, $P(q)$, related to the native PNA crystallographic structure (entry: 2TEP in the Protein Data Bank), was calculated by making use of SASMOL software [27].

3. Results and discussion

3.1. The stability of PNA at physiological pH and room temperature

First of all, we calculated the theoretical SAXS profiles for the tetrameric PNA crystallographic structure, as well as for the monomer and dimer sub-units by means of the SASMOL software [27]. Fig. 1A displays the calculated curves with the corresponding $p(r)$ functions (inset in Fig. 1A). The scattering curve of the tetrameric PNA differs significantly from its sub-units. The SAXS curve presents a well-defined local minimum at $q \sim 0.12$ Å^{-1}, whereas for dimers and monomers the first minimum is displaced to longer q values ($q \sim 0.2$ Å^{-1}, Fig. 1A). Noteworthy, all associations of monomers into dimers generate similar scattering curves (data not shown). Then, just a representative dimer is drawn in Fig. 1A. One should also notice that the increase in the forward scattering intensity, $I(q \to 0)$, is due to differences on the monomer, dimer and tetramer volumes. Furthermore, from the corresponding normalized $p(r)$ functions (inset in Fig. 1A), the dimer and tetramer maximum dimensions, D_{max}, are 80 Å, whereas D_{max} decreases to circa 50 Å for the monomer sub-unit (arrows in the bottom of the inset, Fig. 1A). The maximum frequency of distances occurring inside the scattering particle diminishes from circa 41 Å to 24 Å and 20 Å (arrows in the top of the inset, Fig. 1A) as the protein dissociates from the tetramer to the dimer and to the monomer, respectively. The calculated R_g values for monomers, dimers and tetramers are, respectively, 16.7 Å, 25.4 Å and 29.2 Å.

The PNA experimental data at pH 7.4 (open circles) along with the best model-free fitting (dashed-line) obtained by GIFT software [26] and the calculated curve for the homotetramer PNA crystallographic structure (solid line) are shown in Fig. 1B. As one can see, the calculated scattering curve reproduces quite well the experimental data (Fig. 1B). Besides, $p(r)$ function simulated through the model-free methodology by means of GIFT software (dashed line) is quite similar to that calculated from the PNA structure (solid line in the inset in Fig. 1B). The maximum frequency of distances inside the scattering particle and D_{max} values extracted from the $p(r)$ functions amount to 41 Å and 80 Å, respectively. Therefore, our results give support to conclude that PNA in buffer solution, at pH 7.4, is

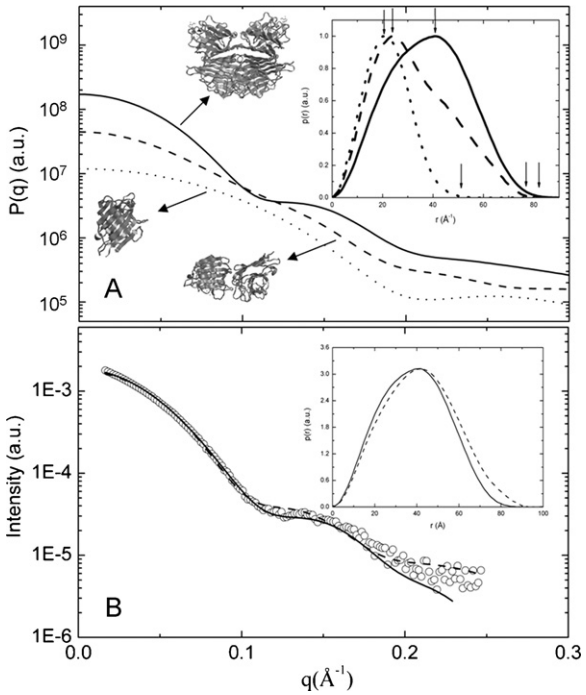

Fig. 1. SAXS curves of native PNA. (A) SAXS curves of homotetramer PNA structure (solid line), dimer (dashed line) and monomer (dotted line) subunits, calculated from the protein crystallographic structure (PDB entry: 2TEP) and the corresponding $p(r)$ functions (inset) using SASMOL software [27]. (B) SAXS curve of PNA at pH 7.4 (open circles) with the best fit (dashed line) calculated with GIFT software [26] and the theoretical curve (solid line) from the crystallographic structure by means of SASMOL [27], and the corresponding $p(r)$ functions (inset).

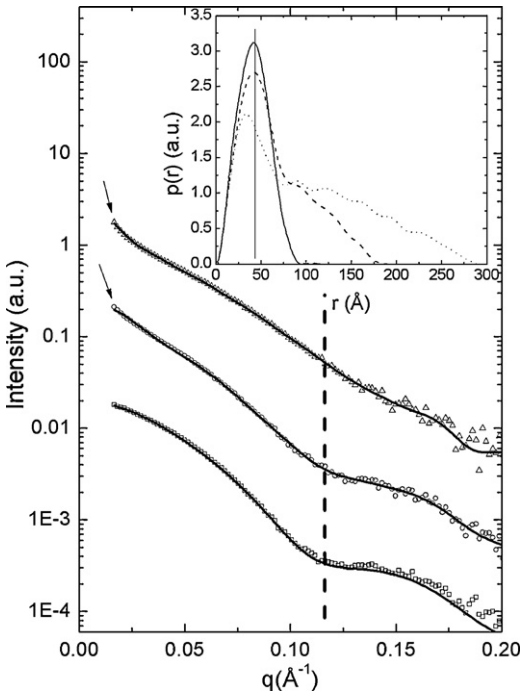

Fig. 2. PNA SAXS curves at pH variation. Small angle X-ray scattering curves of PNA at pH 2.5 (open triangles), 4.0 (open circles) and 9.0 (open squares), and the best fittings (solid lines) corresponding to the $p(r)$ functions (dotted, dashed and solid lines, respectively, in the inset) obtained through GIFT procedure [26].

a homotetrameric lectin in a jelly roll structure as it was found in the native crystallographic structure [17].

Previous dynamic light scattering (DLS) measurements of PNA at pH 7.0, in 20 mM phosphate buffer solution and 150 mM NaCl, showed that the protein has a globular shape with hydrodynamic radius equals to $R = 39$ Å [19]. Such a value is compatible with the radius of gyration of 29.2 Å found here ($R_g = \sqrt{3/5}R$) [25]. Furthermore, molecular dynamics simulations on the thermal PNA denaturation reported on $R_g = 29.5$ Å [28], also in agreement with our results. A similar R_g value was also recently determined by SAXS to camptosemin that is another tetrameric lectin [23].

With the aim of better understanding the stability of PNA quaternary structure, the protein was submitted to pH variation, as follows.

3.2. Stability of PNA at different pH and room temperature

The stability of PNA quaternary structure was investigated at acid and basic pH values (2.5, 4.0 and 9.0). Fig. 2 shows the SAXS data for PNA at pH 2.5 (open triangles), 4.0 (open circles) and 9.0 (open squares). At pH 9.0, the scattering curve is identical to that of pH 7.4 (Fig. 1B). Therefore, PNA keeps its quaternary conformation, at room temperature, from physiological to basic environment up to pH = 9.0. In contrast, when pH values decrease to acid range, the conformation starts to change as we describe below.

Fig. 2 shows the best fittings obtained with GIFT software for PNA in buffer solution and the corresponding $p(r)$ functions for all studied pH range (inset in Fig. 2). The scattering curves are displaced for clarity. At pH 4.0, the SAXS curve is similar to that of pH 9.0 with the prevalence of a minimum around 0.12 Å^{-1}. However, there is a small upturn in the intensity at low q values (arrow in Fig. 2) that is related to the scattering of some protein aggregates in solution [29,30]. The $p(r)$ function displays a first shoulder at $r = 41$ Å similarly to that found at pH 7.4 (Fig. 1) and 9.0 (Fig. 2). D_{max} extends to circa 170 Å due to the protein aggregation process. Note that there is a decrease in $p(r)$ magnitude at r values smaller than ~70 Å in respect to that observed at pH 7.4 and 9.0, due to a decrease of the tetrameric population into a favor of multimeric species in solution. Therefore, our results point out that the homotetrameric structure is the predominant PNA form at pH 4.0, although some aggregates coexist in buffer solution at room temperature.

On the other hand, the maximum of frequencies in the $p(r)$ function decreases from 41 Å to 34 Å at pH 2.5 (inset in Fig. 2) that can be related to a partial dissociation of the tetrameric unit into monomers and dimers. At the same time, there is a significant amount of distances larger than 100 Å inside the scattering particle, reaching D_{max} at circa 300 Å. Such an increase is due to the formation of protein aggregates in solution that give rise to the upturn in the scattering intensity at low q values (arrow in Fig. 2). The minimum at $q \sim 0.12$ Å^{-1} in the SAXS curve disappears (Fig. 2). The Kratky plot confirms that the scattering particles are still compact, with no protein unfolded profile (data not shown) [30,22]. Taking together and comparing the results with the theoretical calculations displayed in Fig. 1, the SAXS results evidence that PNA is under a dissociation process at pH 2.5, accompanied by a reassembling of the sub-units into larger aggregates.

Therefore, although PNA keeps most of its quaternary structure at room temperature and pH 4.0, we can infer that the conformational stability is different as compared to PNA in a physiological and basic environment, once a beginning of aggregation process takes place. The conformational instability is pronounced at pH 2.5. The instability of other lectins at pH 2.5 has already been reported in the literature, with the dissociation of tetramers to monomers for camptosemin [23] and soybean agglutinin [31].

In what follows, we submitted PNA to temperature variation and high amounts of GndHCl.

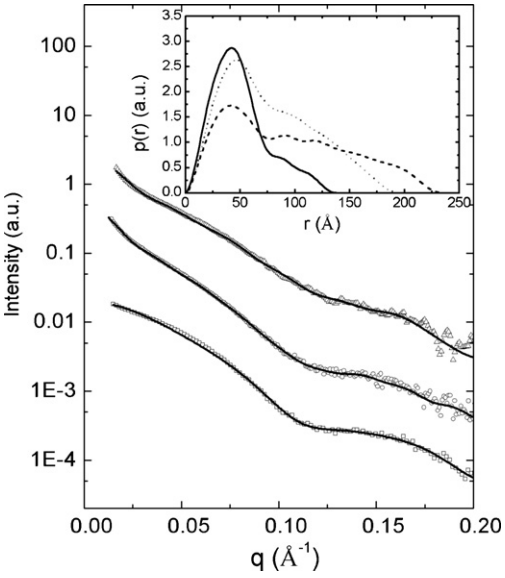

Fig. 3. PNA SAXS curves at 45 °C and pH variation. Small angle X-ray scattering curves of PNA at pH 7.4 (open squares), 9.0 (open circles), and 4.0 (open triangles). The best fitting obtained through GIFT procedure [26] are displayed as solid lines. The inset shows the corresponding $p(r)$ functions for PNA at pH 7.4 (solid line), 9.0 (dotted line), and 4.0 (dashed line).

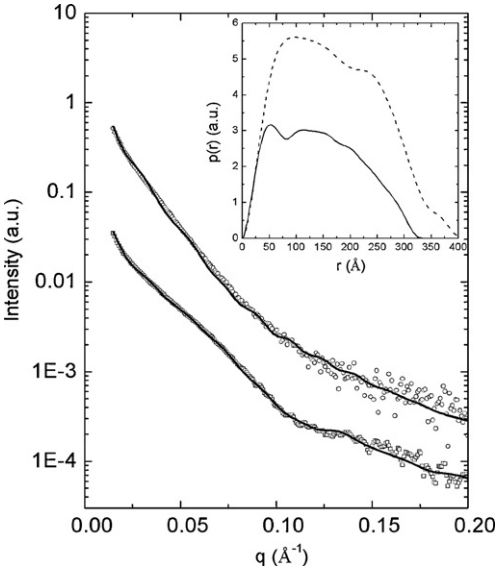

Fig. 4. PNA SAXS curves at 60 °C and pH variation. Small angle X-ray scattering curves of PNA at temperature of 60 °C at pH 7.4 (open squares) and 9.0 (open circles), with the best fitting obtained through GIFT procedure [26] displayed as solid lines. The inset shows the corresponding $p(r)$ functions for PNA at pH 7.4 (solid line) and 9.0 (dashed line).

3.3. Temperature stability under pH variation

Fig. 3 shows the SAXS curves of PNA at temperature of 45 °C and pH 7.4 (open squares), 9.0 (open circles) and 4.0 (open triangles). At pH 2.5 and temperature of 35 °C, a beginning of sample precipitation was observed. Such a precipitation process became complete at 45 °C. Therefore, the combined effect of temperature and acid pH induces a quick formation of large PNA aggregates that ends up to immediate PNA precipitation.

At pH 7.4, the homotetrameric PNA conformation is still stable at 45 °C, although the scattering of some larger aggregates starts to influence the SAXS curve at low q values, also reflected by the D_{max} value in the corresponding $p(r)$ function (Fig. 3). The coexistence of tetramers and larger aggregates of PNA in buffer solution is even more pronounced at pH 9.0 (Fig. 3).

At pH 4.0 and temperature of 45 °C, partial protein precipitation was observed, evidencing some instability of the protein quaternary structure under this condition. Note that there is a significant upturn in the scattering intensity at low q values (Fig. 3) that leads to an increase in D_{max} to circa 230 Å, whereas the magnitude of $p(r)$ function corresponding to tetrameric structure diminishes. Then, the SAXS results (Fig. 3) reveal the formation of larger aggregates coexisting with a smaller amount of tetramer species at pH 4.0 in respect to those present at neutral and basic environments at T = 45 °C. The protein became very instable by heating the sample up to 60 °C, where a complete sample precipitation occurred.

Regarding the conformational stability of the protein at neutral and basic environment under temperature increasing, Fig. 4 shows the SAXS curves of PNA at 60 °C and pH 7.4 (open squares) and 9.0 (open circles).

As one can see, the SAXS curves present quite different profiles in respect to those displayed at lower temperatures. The corresponding $p(r)$ functions demonstrate that, at pH 7.4, there are still tetramers in solution as inferred by the presence of maximum frequencies around 41 Å, coexisting with a significant population of multimeric species. The tetramers species disappear at pH 9.0, as evidenced by the changes observed in the SAXS profile and $p(r)$ function, which are typical from the scattering of larger aggregates in solution [32]. Therefore, although PNA at pH 7.4 and 9.0 is assembled in a tetrameric structure at 25 °C, it responds differently to the temperature effect.

3.4. Stability at GndHCl presence at pH variation

The addition of GndHCl 0.5 M at pH 2.5 leads to the formation of large aggregates as evidenced by sample precipitation. In contrast, the presence of the same amount of GndHCl does not induce the PNA precipitation at pH 4.0, 7.4 and 9.0. Such effect emphasizes indeed the very low stability of PNA quaternary structure at pH 2.5, as also evidenced by temperature increase.

To enlighten the results, Fig. 5 shows the SAXS curves of PNA at pH 4.0, 9.0 and 7.4, in the presence of 0.5 (Fig. 5A) and 2.0 M (Fig. 5B) of GndHCl, respectively.

The scattering curves for PNA at pH 7.4 and 9.0 in the presence of 0.5 M of GndHCl are quite similar to that of PNA in the guanidine-free solution (Fig. 1). The main difference resides in the beginning of the SAXS curves in the presence of 0.5 M denaturating agent, once the upturn in the intensity reflects the formation of some aggregates into a larger extent at pH 9.0. So, most of the proteins in solution have the same native quaternary structure probably coexisting with some oligomers.

Concerning PNA at pH 4.0, the presence of GndHCl 0.5 M affects the protein quaternary conformation. According to the previous analysis, PNA must undergo to a dissociation process followed by an aggregation of the sub-units, noticed by changes in the scattering curve profile (Fig. 5A).

Under the influence of GndHCl 2.0 M (Fig. 5B), the presence of a minimum around 0.12 Å^{-1} still indicates that PNA at pH 7.4 must coexist as native (i.e., in the tetrameric form) and oligomeric forms. On the other hand, at pH 4.0 and 9.0, the minima in the scattering curves are smoothed and the intensity upturns at low q values are quite accentuated. Therefore, our results demonstrate that the protein becomes instable at acid and basic environment, with the formation of some larger aggregates in solution.

Finally, it is clear from the guanidine experiments that PNA has a more stable quaternary conformation at physiological pH. PNA also shows some stability (but not equal to pH 7.4) at pH 9.0. Such conformational stability, however, decreases at acidic pH (4.0 and

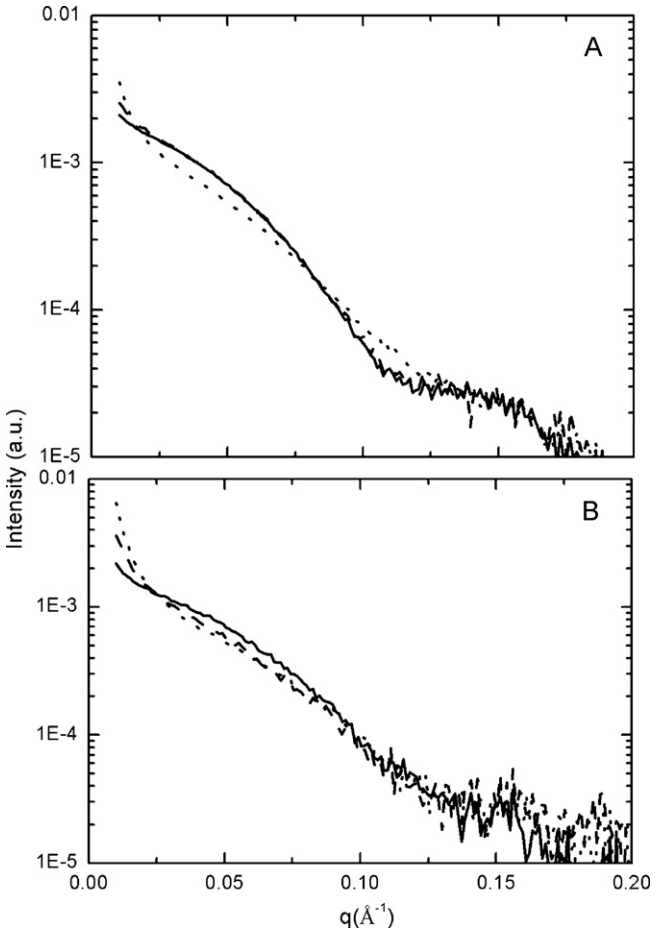

Fig. 5. PNA at GndHCl variation. SAXS curves in the presence of 0.5 (A) and 2.0 M (B) of GndHCl at pH 7.4 (solid lines), 9.0 (dashed lines) and 4.0 (dotted lines).

2.5). At pH 2.5 the protein has the smallest stability as compared to pH 7.4, 9.0 and 4.0, being strongly affected by GndHCl 0.5 M.

3.5. Stability at T-antigen presence

For understanding the sugar binding role at PNA quaternary stability, all experiments were also performed in the presence of T-antigen. It was observed that this sugar does not affect the conformational stability neither at pH and temperature variation, nor upon GndHCl addition (results not shown). On the other hand, X-ray diffraction experiments have demonstrated that PNA crystals can grow at low pH (typically 4.5) when a sugar or peptide sequence is bound [17,33], suggesting that the sugar binding region is highly flexible. Such a flexibility allows the protein crystals to grow in different environmental conditions, and changes near to these regions have, generally, a small effect. The results presented here are in accordance to this statement, and are also consistent with the structural variability exhibited by the β sheets involved at quaternary folding [17], not being affected by the small changes caused by T-antigen presence.

4. Conclusions

In this work we studied the stability of PNA at different pH values, temperatures and GndHCl amount by means of SAXS. Interestingly, at room temperature and physiological and basic environments, the protein presents the same structural conformation. Nevertheless, PNA behaves differently under thermal stress at each studied pH, suggesting that the protein stability is not only structurally driven, but also pH-dependent. The presence of T-antigen does not alter the SAXS curve profile, indicating that T-antigen is not able to promote significant protein structure modifications. Nevertheless, one should notice that SAXS is a small resolution technique and local or small changes on the protein structure could not be evidenced.

Acknowledgements

The authors are in debt with Prof. Dr. Paolo Mariani and Francesco Spinozzi from *Università Politecnica delle Marche*, Ancona, Italy to provide SASMOL software. Authors are grateful to Fundação de Amparo à Pesquisa do Estado de São Paulo (FAPESP) for financial support, and to Laboratório Nacional de Luz Síncrotron (LNLS) for SAXS measurements. RI is grateful to Conselho Nacional de Desenvolvimento Científico e Tecnológico (CNPq).

References

[1] P. Garred, Biochem. Soc. Trans. 26 (6) (2008) 1461–1466.
[2] H. Lis, N. Sharon, Chem. Rev. 98 (1998) 637–674.
[3] J. Balzarini, K. Van Laethem, S. Hatse, M. Froeyen, W. Peumans, E. Van Damme, D. Schols, JBC 280 (49) (2005) 41005–41009.
[4] D.B. Williams, J. Cell Sci. 119 (4) (2006) 615–623.
[5] S. Dev, S. Sinha, A. Surolia, IUBMB Life 58 (9) (2006) 549–555.
[6] F. Naseem, R.H. Khan, BBA 1723 (1–3) (2005) 192–200.
[7] P.T. Campana, D.I. Moraes, A.C.O. Monteiro-Moreira, L.M. Beltramini, Eur. J. Biochem. 269 (2002) 753–758.
[8] M.E. Carrizo, S. Capaldi, M. Perduca, F.J. Irazoqui, G.A. Nores, H.L. Monaco, J. Biol. Chem. 280 (11) (2005) 10614–10623.
[9] E. Skutelsky, R. Lotan, N. Sharon, D. Danon, BBA 467 (2) (1977) 165–174.
[10] V. Friedenreich, The Thomsen Hemagglutinin Phenomenon, Levin & Munksgaard, Copenhagen, 1930.
[11] L. Cipolla, F. Peri, C. Airoldi, Anticancer Agents Med. Chem. 8 (2008) 92–121.
[12] D.P. Galonic, D.Y. Gin, Nature 446 (26) (2007) 1000–1007.
[13] M.V.K. Sastry, P. Banarjees, S.R. Patanjalill, M.J. Swamy, G.V. Swarnalatha, A. Surolia, JBC 261 (25) (1986) 11726–11733.
[14] C.R. Boland, Y.F. Chen, S.J. Rinderle, J.H. Resau, G.D. Luk, H.T. Lynch, I.J. Goldstein, Cancer Res. 51 (2) (1991) 657–665.
[15] J. Pramanik, U. Chatterjee, G. Mondal, P.T. Campana, B.P. Chatterjee, Glycobiol. Insights 2 (2010) 83–99.
[16] Y. Cao, P. Stosiek, G.F. Springer, U. Karsten, Histochem. Cell Biol. 106 (1996) 197–207.
[17] R. Bannerjee, K. Das, R. Ravishankar, K. Suguna, A. Surolia, M. Vijayan, J. Mol. Biol. 259 (1996) 281–296.
[18] W.W. Fish, L.M. Hamlim, R.L. Miller, Arch. Biochem. Biophys. 190 (2) (1978) 693–698.
[19] S. Dev, A. Surolia, J. Biosci. 31 (2006) 551–556.
[20] S. Dev1, R.H. Khan, A. Surolia, IUBMB Life 58 (8) (2006) 473–479.
[21] D. Pallarola, N. Queralto, W. Knoll, M. Ceolin, O. Azzaroni, F. Battaglini, Langmuir 26 (16) (2010) 13684–13696.
[22] F.P. Silva Jr., G.M.C Alexandre, C.H.I. Ramos, S.G. De-Simone, Toxicon 52 (2008) 944–953.
[23] F.A.H. Batista, L.S. Goto, W. Garcia, D.I. de Moraes, M.O. Neto, I. Polikarpov, M.R. Cominetti, H.S. Selistre-de-Araújo, L.M. Beltramini, A.P.U. Araújo, Eur. Biophys. J. 39 (2010) 1193–1205.
[24] A. Guinier, G. Fournet, Small Angle Scattering of X-Rays, 1st ed., Wiley, New York, 1955.
[25] O. Glatter, O. Kratky, Small Angle X-ray Scattering, 1st ed., Academic Press, London, 1982.
[26] A. Bergmann, G. Fritz, O. Glatter, J. Appl. Cryst. 33 (2000) 1212–1216.
[27] M.G. Ortore, F. Spinozzi, P. Mariani, A. Panciaroni, L.R.S. Barbosa, H. Amenitsch, M. Teinhart, J. Oliver, J. R. Soc. Interface 6 (2009) 619–634.
[28] P. Hansia, S. Dev, A. Surolia, S. Vishveshwara, Proteins 69 (2007) 32–42.
[29] L. Mourey, J.-D. Pédelacq, C. Fabre, H. Causse, P. Rougé, J.-P. Samama, Proteins Struct. Funct. Genet. 29 (1997) 433–442.
[30] K.S. Jin, Y. Rho, J. Kim, H. Kim, I.J. Kim, M. Ree, J. Phys. Chem. B 112 (2008) 15821–15827.
[31] S. Sinha, A. Surolia, Biophys. J. 88 (2005) 4243–4251.
[32] D. Lehner, P. Worning, G. Fritz, L. Ogendal, R. Bauer, O. Glatter, J. Colloid Interface Sci. 213 (1999) 445–456.
[33] S.K. Natchiar, A.A. Jeyaprakash, T.N.C. Ramya, C.J. Thomas, K. Suguna, A. Surolia, M. Vijayan, Acta Cryst. D 60 (2004) 211–219.